Short Communication

Nitrogen Doped Carbon Wrapped Fe₃O₄ as an Efficient Bifunctional Oxygen Electrocatalyst

Zhijia Zhang, Qiao Shu[*], *Chan Chen, Tianci Xiao, Zhiyi Hu, Shuaicheng Wu and Junsheng Li*[*]

School of Chemistry, Chemical Engineering and Life Sciences, Wuhan University of Technology, Luoshi Road 122#, Wuhan, P. R. China
[*]E-mail: 1756799511@qq.com, li_j@whut.edu.cn

The development of green energy conversion devices such as metal air battery relies on the use of efficient reversible oxygen electrocatalyst. Commonly used precious metal catalyst could not support the large scale application of these devices due to their high cost and limited stability. In this paper, we report the synthesis of a coordination polymer and its use for the preparation of oxygen electrocatalyst. Our results show that the use of the coordination polymer as catalyst precursor could results in a homogeneous catalyst with both high activity and good stability, which is close to that of commercial Pt/C catalyst. Our results show that the nitrogen doped carbon wrapped Fe_3O_4 could function as a promising oxygen catalyst in a variety of applications.

1. INTRODUCTION

The quest of replacing traditional fossil fuel with green energy sources has significantly stimulated the development of novel energy conversion devices. Metal air battery and proton exchange membrane fuel cell has emerged decades ago and are demonstrated to hold high potential for practical applications such as electric vehicles. Despite the advancement of these devices, the efficiency of these devices is still to be improved. This is due to the fact that the kinetics of oxygen reduction reaction (ORR) and oxygen evolution reaction (OER), which are involved in the working process of these devices, are intrinsically slow.[1, 2] Therefore, it is critical to develop high-performance oxygen electrode catalyst in order to enhance the performance of these electrochemical devices.[3]

Precious metal based electrocatalysts have been widely used to catalyze ORR and OER. However, the scarcity as well as the high cost of the precious metal electrocatalyst hindered their large

scale use. Moreover, precious metal electrocatalyst is susceptible to poisons and thus show poor stability. Metal oxide based electrocatalyst is an alternative oxygen electrocatalyst that has low cost and promising catalytic activity.[4-10] Their catalytic activity of the transition metal oxides can be enhanced to the level comparable to precious metal catalyst by engineering their composition and electronic state. To further improve their catalytic performance, transition metal oxides were composited with different carbon materials.[11-13] In such a composite, the carbon phase on one hand provides conductive pathways for the electron transport in the ORR/OER process. On the other hand, the carbon phase itself may effectively catalyze ORR/OER, further increasing the performance of the composite. More importantly, there might exist a synergy between the metal oxide and the carbon phase and this synergy can boost the efficiency of the composite catalyst. Traditionally, such a composite was prepared by carbonization of a mixture containing metal precursor and carbon precursor[11] or post modification of metal oxide with carbon phase[14]. These methods suffer from either their poor ability to control the dispersion of active sites or complicated fabrication process. Herein, we report a facile synthesis of nitrogen doped carbon wrapped Fe_2O_3 bifunctional oxygen electrocatalyst through direct carbonization of a coordination polymer. The as-produced catalyst shows high ORR/OER performance and good stability. Moreover, the synthetic method can be generalized to the preparation of other metal oxide@C composite.

2. EXPERIMENTAL

Synthesis of the coordination polymer precursor. 660 mg of poly(vinylpyrrolidone) (PVP) was dissolved in 88 mL deionized water. Next, 2 mL $FeCl_3$ solution (100 mg mL^{-1}) was added into the PVP solution and stirred for 1 h. After stirring, 10 mL (100 mg mL^{-1}) gallic acid (GA) was added to above mixture and stirred overnight to obtain the coordination polymer. The coordination polymer was purified by dialysis of the crude product (MWCO 25000) against deionized water for 48 h. The purified polymer was dried at 60 °C in an oven. A series coordination polymer with different metal ions were prepared simply by replacing the $FeCl_3$ with corresponding metal salts.

Synthesis of the electrocatalyst. The electrocatalyst was synthesized by carbonization of the coordination polymer under an Ar flow at 800 °C for 3 h (ramping rate 5 °C min^{-1}). The carbonization yield was ~20%, determined by weighing. The carbonization product was washed with 0.5 M HCl to remove the unbounded Fe species in the product.

Characterizations. The morphology of the product was characterized with SEM (JSM-IT300, JEOL) and TEM (Tecnai G2 F20 S-TWIN) measurements. The composition of the product was studied with a XRD meter (D/MAX-RB RU-200B, Rigaku) equipped with a Cu Kα source. All the electrochemical characterizations were conducted with a three-electrode configuration in O_2 saturated 0.1 M KOH solution using Pt foil electrode, Ag/AgCl electrode and glassy carbon electrode as the counter electrode, reference electrode and working electrode, respectively. All the potential in this paper was converted to RHE scale using the following equation: $E_{RHE} = E_{Ag/AgCl} + 0.0591 \times pH + 0.197$. To prepare the catalyst ink, 4 mg catalyst was dispersed in a mixture solution containing 20 μL Nafion solution, 100 μL deionized water and 900 μL isopropanol.

The catalyst ink was sonicated to ensure a homogeneous dispersion of catalyst in the ink. To prepare the working electrode, 20 µL of the catalyst was dropped onto the glassy carbon electrode and the electrode was left in air to dry naturally. CV measurements were carried out in the potential range of 0.1649 V to 1.1649 V with a scan rate of 50 mV s^{-1}. ORR LSV tests were performed in a potential range of 1.1649 V to 0.1649 V and OER LSV curve was conducted from 1.0649 V to 1.9649 V. The sweep rate for LSV measurement is 10 mV s^{-1}.

3. RESULTS AND DISCUSSION
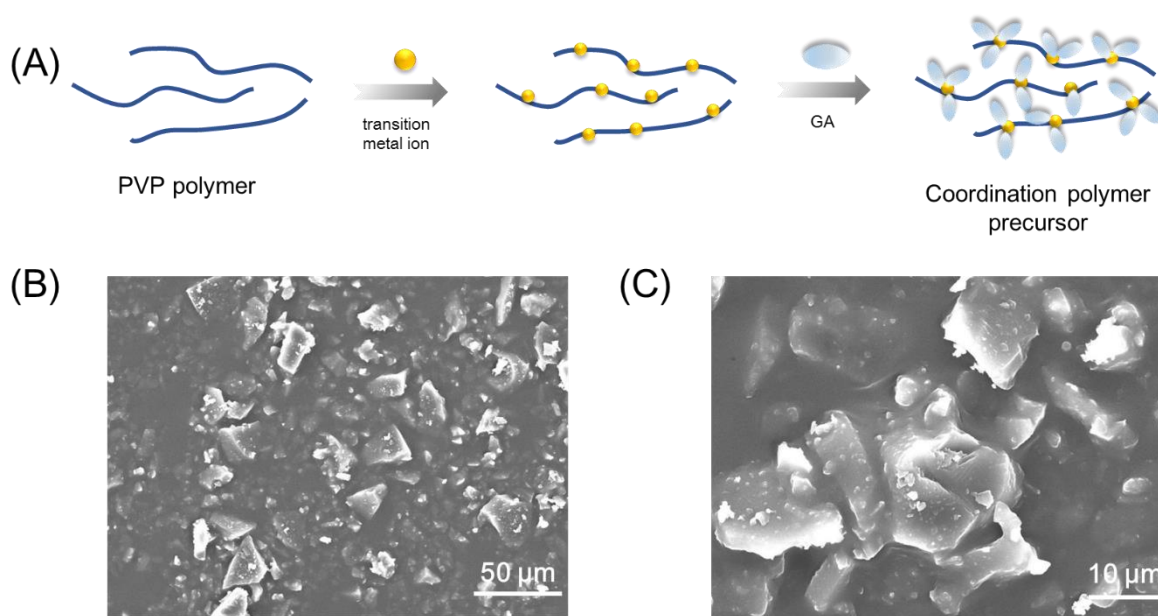
Figure 1. (A) Schematic illustration of the preparation process of the coordination polymer precursor. (B, C) SEM images of Fe-N-C-800 at different magnifications.

The schematic illustration for the synthesis of the coordination polymer precursor is shown in Fig. 1A. Fe containing coordination polymer was synthesized by mixing poly(vinylpyrrolidone) (PVP) solution, FeCl$_3$ and gallic acid (GA). PVP serves as the carbon and nitrogen sources for the synthesis of the catalyst. Upon mixing with PVP, Fe^{3+} assembled onto backbone of PVP through electrostatic self-assembly.[15] Due to the high affinity between phenols and transition metal ions[16], subsequent addition of GA would lead to instant formation of GA-Fe^{3+} complex. The GA-Fe^{3+} complex could inhibit the aggregation of PVP polymer, thereby leading to the generation of a coordination polymer with uniform distribution of Fe and N species. The homogeneous dispersion of Fe and N species is particularly beneficial for the sufficient utilization of active sites in the resulting catalyst. The obtained coordination polymer was then dried and carbonized in N$_2$ atmosphere at 800 °C. The products were denoted as Fe-N-C-800 in the following. The morphology of Fe-N-C-800 was first studied with SEM tests. The catalyst exhibited a monolith morphology with nanoscale roughness (Fig. 1B, C). To further probe the morphology of the catalyst, TEM characterizations were performed (Fig. 2A). It can be

clearly seen that nanoparticles of Fe species (dark particles) were homogeneously dispersed in carbon matrix and nanoparticles of iron species were closely wrapped within the carbon matrix. Although the nanoparticle is not in direct contact with the reactants during ORR process, the nanoparticle may activate the surrounding carbon phase by decreasing the local work function of surrounding carbon[17], thus improving the overall ORR activity of the composite. The composition of Fe-N-C-800 was studied with XRD measurements. As shown in the XRD pattern (Fig. 2B), a broad peak centered at ~25°, which can be ascribed to the (002) peak of graphite, was observed. In addition, characteristic peak from Fe_3O_4 was also present, confirming that Fe-N-C-800 was composed of graphite carbon and Fe_3O_4. Since PVP and GA can coordinate with a number of transition metal ions, the current method could be extended for the preparation of a series of metal oxide-carbon catalyst. To demonstrate this, Ni-N-C-800, Mn-N-C-800 and Co-N-C-800 were also synthesized.
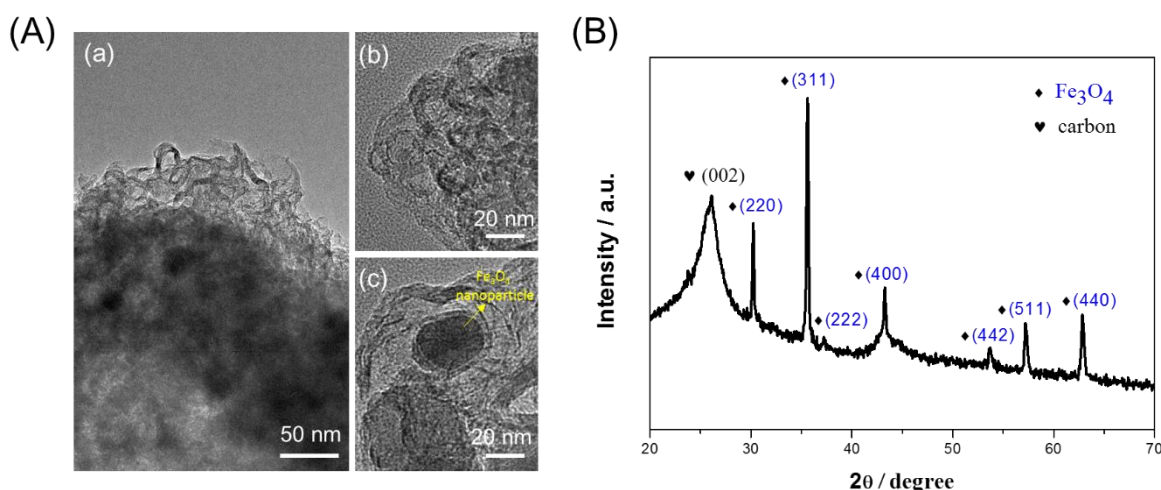
Figure 2. (A) TEM image of Fe-N-C-800. (B) XRD spectra of Fe-N-C-800.
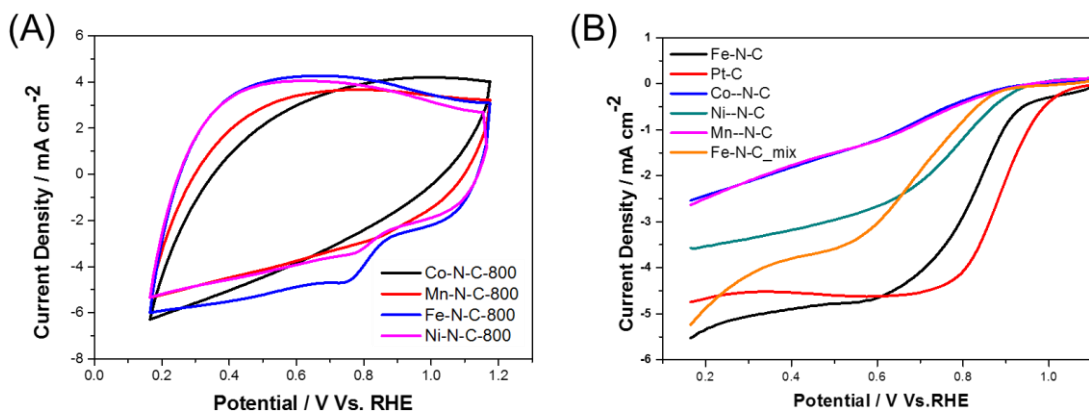
Figure 3. (A) CV curves of Co-N-C-800, Mn-N-C-800, Fe-N-C-800 and Ni-N-C-800 in O_2 saturated 0.1M KOH. (B) LSV curve of Pt/C, Co-N-C-800, Mn-N-C-800, Fe-N-C-800, Fe-N-C_mix and Ni-N-C-800 in O_2 saturated 0.1 M KOH at a rotating speed of 1600 rpm.

The electrochemical performance of the as-synthesized catalysts was first investigated with CV tests (Fig. 3A). The CV curves of Fe-N-C-800, Ni-N-C-800, Mn-N-C-800 and Co-N-C-800 showed ORR reaction current. The ORR activity of the catalyst can be reflected by the ORR reaction current.[18] Therefore, Fe-N-C-800, which showed the highest reaction current in the CV measurement, had the best ORR activity among the M-N-C-800 catalysts. No excess peak was observed in the CV curves, demonstrating the good stability of these catalysts. To further investigate the ORR performance of the catalysts, LSV measurements were conducted (Fig. 3B). As depicted in the figure, the ORR performance changed in the following order: Co-N-C-800≈Mn-N-C-800<Ni-N-C-800<Fe-N-C-800. Among the M-N-C catalyst, Fe-N-C-800 had a comparable ORR onset potential (0.99 V Vs. RHE) with 20% Pt/C catalyst (1.02 V). In addition, the limiting current density of Fe-N-C-800 was also close to that of Pt/C catalyst. Such a high ORR activity of Fe-N-C-800 is comparable to some of the novel ORR electrocatalysts reported recently.[19-22] To probe the ORR mechanism on the catalyst, the LSV curves of the catalysts at different rotating speeds ranging from 400 rpm to 2000 rpm was recorded and the electron transfer number of the catalysts under different potential were calculated (Fig. 4A). The electron transfer number was calculated to be ~4 in the potential range of 0.25 V to 0.70 V. These results suggested that ORR on Fe-N-C-800 proceeded through a quasi-four electron process, which is highly favorable in ORR catalytic reactions.[23] To prove the effect of the coordination process on the performance of the resulting product, a solid mixture comprising of the same amount of $FeCl_3$, PVP and GA with that in the coordination polymer precursor was produced and used as precursor to generate electrocatalyst (denoted as Fe-N-C_mix). LSV results showed that Fe-N-C_mix had a more negative onset potential and a lower limiting current density than Fe-N-C-800 (Fig. 3B). The enhanced performance of Fe-N-C-800 could be largely attributed to the improved dispersion of Fe and N species in the catalyst. Fe and N species are potential ORR active phases in the resulting catalyst.[23, 24] Therefore, homogeneous distribution of Fe and N species is beneficial for the exposure of these active sites and thus maximizing the catalytic activity of the resulting catalyst.[25] Moreover, Fe element and N element in the complex precursor is close to each other. Such a configuration may enable the generation of Fe-N coordination species, which can further enhance the overall ORR performance,[26] during the carbonization process. Due to the combination of these merits, the Fe-N-C-800 catalysts synthesized from the complex precursor showed a superior ORR performance. The stability of the electrocatalyst under ORR conditions was also evaluated by chronoamperometric test at 0.6649 V (Vs. RHE). Current retention of the electrocatalyst, defined as the ratio between ORR reaction current at a certain time point and its initial ORR reaction current, was recorded to characterize the stability of the electrocatalyst. Fe-N-C-800 showed similar performance decay rate with 20% Pt/C catalyst at this condition and the ORR reaction current of Fe-N-C-800 decreased by ~17.1% after 10000 s test. In contrast, Fe-N-C_mix showed poor durability under identical condition and the current density retention is only 48.3%.
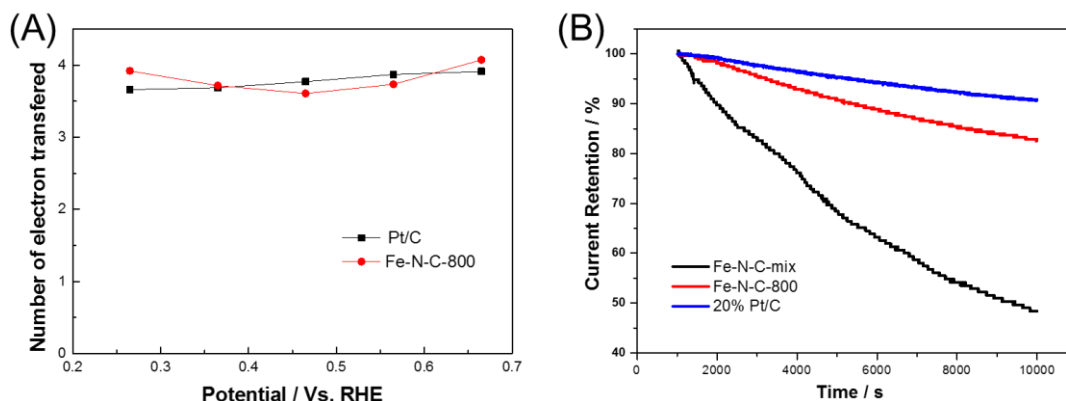
Figure 4. (A) Electron transfer number of Fe-N-C-800 and Pt/C. (B) ORR current retention of Fe-N-C-800, Fe-N-C_mix and Pt/C in O_2 saturated 0.1M KOH at a rotating speed of 1600 rpm.

The poor stability of Fe-N-C_mix is most likely to be originated from its inhomogeneous distribution of the ORR active sites within the catalyst. Next, the OER performance of the catalysts were evaluated by LSV measurement in the potential range of 1.0649 V to 1.9649 V (Vs. RHE). Fe-N-C-800 again showed the best OER performance among the M-N-C-800 catalysts. The high OER activity of Fe-N-C-800 can be explained by its unique morphology and composition. The potential required to achieve an OER current density of 10 mA cm^{-2} was ~1.93 V (Vs. RHE). 20% Pt/C possessed a similar OER activity with that of Fe-N-C-800. The potential gap between the potential with an OER current of 10 mA cm^{-2} and ORR half wave potential was normally used to quantify the reversible oxygen catalytic activity of the catalyst.[27] Here, the potential gap of Fe-N-C-800 was calculated to be 1.10 V, close to that of 1.05 V for 20% Pt/C and some metal oxide electrocatalyst reported recently.[28]
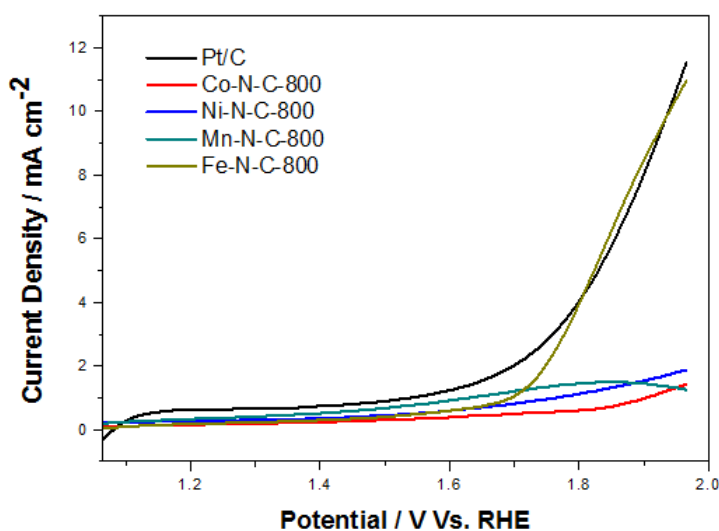
Figure 5. LSV curves of Pt/C, Co-N-C-800, Mn-N-C-800, Fe-N-C-800 and Ni-N-C-800 in O_2 saturated 0.1M KOH at a rotating speed of 1600 rpm.

4. CONCLUSION

In summary, a series of coordination polymers were synthesized and used for the carbonization preparation of reversible oxygen electrocatalyst. Among the synthesized catalyst, Fe-N-C-800 showed a highest ORR and OER activity that is similar to 20% Pt/C catalyst. XRD results show that Fe-N-C-800 is composed of graphite carbon and Fe_3O_4. In addition, morphology characterizations demonstrate that Fe_3O_4 phase is closely wrapped within the carbon matrix. Such a unique morphology may contribute to its high catalytic activity. Our results suggest that the carbon wrapped Fe_3O_4 catalyst reported herein could serve as a potential candidate for fuel cell and metal air battery application. In addition, the synthetic method used here could be used as a general approach toward functional metal oxide materials.

References

1. Z. H. Xia, L. An, P. K. Chen and D. G. Xia, *Adv. Energy Mater.*, 6, (2016), 1600458.
2. Z.-L. Wang, D. Xu, J.-J. Xu and X.-B. Zhang, *Chem. Soc. Rev.*, 43, (2014), 7746.
3. M. H. Shao, Q. W. Chang, J. P. Dodelet and R. Chenitz, *Chem. Rev.*, 116, (2016), 3594.
4. K. L. Pickrahn, S. W. Park, Y. Gorlin, H.-B.-R. Lee, T. F. Jaramillo and S. F. Bent, *Adv. Energy Mater.*, 2, (2012), 1269.
5. G. Zhang, B. Y. Xia, C. Xiao, L. Yu, X. Wang, Y. Xie and X. W. Lou, *Angew. Chem. Int. Edit.*, 52, (2013), 8643.
6. X. Han, T. Zhang, J. Du, F. Cheng and J. Chen, *Chem. Sci.*, 4, (2013), 368.
7. J. Xu, P. Gao and T. S. Zhao, *Energ. Environ. Sci.*, 5, (2012), 5333.
8. X. Gao, H. Zhang, Q. Li, X. Yu, Z. Hong, X. Zhang, C. Liang and Z. Lin, *Angew. Chem. Int. Edit.*, 128, (2016), 6398.
9. J. Xu, L. Shi, C. Liang, H. Wu, J. Lei, D. Liu, D. Qu, Z. Xie, J. Li and H. Tang, *ChemElectroChem*, DOI: 10.1002/celc.201700049, (2017).
10. W. T. Hong, M. Risch, K. A. Stoerzinger, A. Grimaud, J. Suntivich and Y. Shao-Horn, *Energ. Environ. Sci.*, 8, (2015), 1404.
11. Y. Tan, C. Xu, G. Chen, X. Fang, N. Zheng and Q. Xie, *Adv. Funct. Mater.*, 22, (2012), 4584.
12. S. Guo, S. Zhang, L. Wu and S. Sun, *Angew. Chem. Int. Edit.*, 51, (2012), 11770.
13. J. Liu, S. Zhao, C. Li, M. Yang, Y. Yang, Y. Liu, Y. Lifshitz, S.-T. Lee and Z. Kang, *Adv. Energy Mater.*, 6, (2016), 1502039.
14. X. M. Ge, Y. Y. Liu, F. W. T. Goh, T. S. A. Hor, Y. Zong, P. Xiao, Z. Zhang, S. H. Lim, B. Li, X. Wang and Z. L. Liu, *ACS Appl. Mat. Interfaces*, 6, (2014), 12684.
15. F. Liu, X. He, H. Chen, J. Zhang, H. Zhang and Z. Wang, *Nat. Commun.*, 6, (2015), 9003.
16. H. Ejima, J. J. Richardson, K. Liang, J. P. Best, M. P. van Koeverden, G. K. Such, J. W. Cui and F. Caruso, *Science*, 341, (2013), 154.
17. D. Deng, L. Yu, X. Chen, G. Wang, L. Jin, X. Pan, J. Deng, G. Sun and X. Bao, *Angew. Chem. Int. Edit.*, 52, (2013), 371.
18. J. W. Liang, M. Hassan, D. S. Zhu, L. P. Guo and X. J. Bo, *J. Colloid Interf. Sci.*, 490, (2017),

576.

19.   A. C. Mtukula, J. Shen, X. J. Bo and L. P. Guo, *J. Alloy. Compd.*, 655, (2016), 229.

20.   X. J. Bo, Y. F. Zhang, M. A. Li, A. Nsabimana and L. P. Guo, *J. Power Sources* 288, (2015), 1.

21.   H. L. Tang, Y. Zeng, Y. X. Zeng, R. Wang, S. C. Cai, C. Liao, H. P. Cai, X. H. Lu and P. Tsiakaras, *Appl. Catal. B-environ*, 202, (2017), 550.

22.   P. Zhang, W. M. Tu, R. Wang, S. C. Cai, J. Wu, Q. Yan, H. F. Pan, H. N. Zhang and H. L. Tang, *Int. J. Electrochem. Sci.* , 11, (2016), 10763.

23.   R. Wang, J. S. Li, S. C. Cai, Y. Zeng, H. N. Zhang, H. P. Cai and H. L. Tang, *Chempluschem*, 81, (2016), 646.

24.   J. Masa, W. Xia, M. Muhler and W. Schuhmann, *Angew. Chem. Int. Edit.*, 54, (2015), 10102.

25.   A. Brouzgou, S. Q. Song, Z. X. Liang and P. Tsiakaras, *Catalysts*, 6, (2016).

26.   U. I. Kramm, M. Lefevre, N. Larouche, D. Schmeisser and J.-P. Dodelet, *J. Am. Chem. Soc.*, 136, (2014), 978.

27.   D. J. Chen, C. Chen, Z. M. Baiyee, Z. P. Shao and F. Ciucci, *Chem. Rev.*, 115, (2015), 9869.

28.   X. C. Cao, W. N. Yan, C. Jin, J. H. Tian, K. Ke and R. Z. Yang, *Electrochim. Acta* 180, (2015), 788.